

Research Article

Polyvinyl Alcohol/Graphene Oxide Nanocomposite Membrane for Highly Efficient Oil/Water Mixture Separation

Maryam Davardoostmanesh[©], Hossein Ahmadzadeh^{*©}

Department of Chemistry, Faculty of Science, Ferdowsi University of Mashhad, Mashhad, Iran E-mail: h.ahmadzadeh@um.ac.ir

Received: 2 August 2023; Revised: 2 October 2023; Accepted: 31 October 2023

Abstract: The growing amount of oily wastewater caused by frequent oil spill accidents poses a severe threat to the ecological environment. Therefore, the development of highly efficient oil/water separation methods is highly necessary. This work reports the preparation of a nanocomposite membrane using graphene oxide (GO)/polyvinyl alcohol (PVA) coated on steel meshes for oil/water mixture separation. PVA firmly anchors GO nanosheets onto the mesh surface through strong hydrogen bonds using glutaraldehyde (GA) as a crosslinker. This nanocomposite membrane exhibited superhydrophilic and underwater superoleophobic properties, with the highest oil contact angle of 158° due to its highly rough structure. The synergistic effects of GO and PVA further improved the superhydrophilicity of the prepared membrane, due to the hydrophilic nature of both GO and PVA. The separation efficiencies and water flux for a variety of oil/water mixtures were above 97.8% and 6000.0 L m⁻² h⁻¹, respectively. The prepared membrane showed excellent chemical resistance under harsh conditions without evident change in its surface wettability. Moreover, its underwater superoleophobicity was maintained after 10 cycles of abrasion testing.

Keywords: nanocomposite membrane, graphene oxide, polyvinyl alcohol, oil/water separation, superhydrophilicity

1. Introduction

Oil pollution caused by industrial activities and frequent oil spill accidents has led to increased oily wastewater. Therefore, the development of high-performance oil/water separation techniques is of great importance [1]. Among various techniques such as skimming [2, 3], in situ burning [4, 5], flotation [6, 7], and adsorption [8, 9], membrane filtrations with superwetting materials have received significant attention in the oil-water separation field [10-12]. The superwetting membranes for the oil/water mixture include superhydrophilic/underwater superoleophobic and superhydrophobic/superoleophilic membranes [11, 13, 14]. These superwetting membranes were prepared by coating various materials on porous two-dimensional meshes and fabrics, which can allow selective removal of one phase from the other phase [15]. Superhydrophilic/underwater superoleophobic filtration materials inspired by fish scales in water have been developed to overcome some drawbacks in superhydrophobic/superoleophilic materials, such as oil fouling and pore blockage [16]. Most current methods for the preparation of underwater superoleophobic filtration materials are inappropriate with respect to complexity, high cost, and poor stability.

Porous stainless steel mesh (SSL) features high permeability, good fouling resistance, mechanical strength, and low cost, making it an ideal candidate as a substrate; its wettability could be changed by modifying surface chemistry [17,

18]. So far, various types of materials, such as metal organic frameworks [19, 20], zeolites [21, 22], and graphene-based materials [23, 24], have been coated onto meshes to produce superhydrophilic-underwater superoleophobic surfaces.

Based on Young's theory [25], the hydrophilic surface in the air shows oleophobicity underwater, and the creation of hierarchical rough structures amplifies hydrophilicity and underwater superoleophobicity. Graphene oxide (GO), as an excellent hydrophilic carbon-based nanomaterial, can be an ideal candidate for the construction of various underwater superoleophobic surfaces [26-29]. The existence of various oxygen functional groups (e.g., hydroxyl, carboxylic, and epoxide) on the surface of GO sheets makes them hydrophilic and facilitates their interaction with various kinds of materials [30]. However, the stability of the GO-modified mesh membranes remains a challenge, so this problem limits their widespread applications. The GO film can be easily detached during the separation process, resulting in the gradual reduction of underwater superoleophobic properties. Directly coating GO onto the mesh surface without any chemical reaction leads to detachment from the surface [26, 31].

Therefore, the development of new strategies for the preparation of robust and stable underwater superoleophobic membranes is of great significance. The successful coating of GO on the surface of SSL has been reported elsewhere [28, 29]. Dai et al. [32] prepared a hybrid mesh-based membrane with underwater superoleophobic properties via a layer-by-layer assembly method using CaCO₃ and GO as building blocks. Jaleh et al. [33] reported the preparation of a superhydrophobic membrane by anodic electrophoretic deposition of GO on steel mesh. After GO deposition, low-temperature thermal annealing was used to reduce GO by decomposing oxygen-containing groups to change it into a superhydrophobic surface.

GO can create various nanocomposites with polymeric materials, increasing the mechanical strength and stability of the membrane [34, 35]. Modification of the membrane with hydrophilic polymeric materials also leads to improvements in membrane fouling resistance and permeability. Yin et al. [36] reported facile fabrication of nanocomposite membranes using GO/polydopamie (PDA) on the surface of steel mesh. PDA contains abundant catechol, hydroxyl, and amine functional groups, which can improve hydrophilicity and the binding force between GO and steel mesh.

In this study, a superwetting membrane was fabricated by creating a GO/polyvinyl alcohol (PVA) composite on the surface of SSL. One of the issues is that SSL has a rigid and inflexible structure, so tightly assembling nanocomposite onto the surface mesh is very difficult. A PVA polymer was used to fix the GO film on the SSL surface using glutaraldehyde (GA) as a crosslinking reagent. It mainly contains abundant hydroxyl functional groups, which can improve the hydrophilicity and water flux in comparison with a pristine membrane. In spite of some crosslinking methods like sol-gel, which result in crackable and non-uniform coatings [37], the mentioned crosslinking method forms a uniform and stable hydrophilic coating on the mesh surface. To the best of our knowledge, the GO/PVA nanocomposite membrane on the surface of SSL has not been applied for oil-water separation.

The modified SSL showed excellent underwater superoleophobicity due to the strong bonding of GO nanosheets on its surface. The resultant mesh also exhibited good stability in harsh conditions without a significant reduction in underwater oleophobicity. Due to the synergistic effects between GO and PVA, the proposed membrane can be efficiently used for oil and water separation.

2. Experimental section

2.1 Materials

Graphite powder (<0.1 mm, >95%) from Fluka, potassium permanganate (KMnO₄, 99%) from BDH, sulfuric acid (H₂SO₄, 95%), sodium nitrate (NaNO₃, 99%), barium chloride (BaCl₂, 99%), silver nitrate (AbNO₃, 99.5%), hydrofluoric acid (HF, 40%), PVA, and GA (50 wt%) were obtained from Merck. All organic liquids were provided by Mojallali.

2.2 Characterization

The morphological properties of the meshes before and after modification were examined by scanning electron microscopy (SEM; Model LEO 1450VP) images. In order to analyze the structural properties of the nanocomposite membrane, the Fourier-transform infrared (FT-IR) spectra of the meshes were recorded using a Thermo Nicolet Avatar 370 FT-IR Spectrometer. The wetting properties of the meshes were measured by an optical contact angle instrument

equipped with a CCD camera by dropping a few microliters of oil onto the mesh surface.

2.3 Membrane preparation

GO was synthesized via modified Hummers' method [8]. Briefly, GO was dispersed in deionized water for 20 minutes at room temperature. Then, 10 wt% PVA was prepared in DI water with gradual heating until totally dissolving in hot water. SSLs (200 mesh) were cut into strips and washed by ultrapure water. Then, the clean SSL was contacted with a pure HF solution to create an active surface. The activated SSL was dipped in the PVA solution and then it was dried. To complete the crosslinking reaction, the PVA-coated SSL was placed in a 2.0 wt% GA solution (HCl as the catalyst) for a couple of minutes [38]. Then, the PVA-coated mesh was dipped in a 0.5 mg/mL GO suspension, and then it was dried.

2.4 Membrane preparation

The oil-water separation was conducted by immobilizing the prepared membrane between two plastic tubes (20 mm in inner diameter). Before each separation, the membranes were wetted with distilled water. Then, a 1:2 volume ratio of the oil/water mixture was slowly poured onto the membrane and permeated by gravity-driven force until complete separation. The separation efficiency (% η) and water flux (F_w) of the prepared membrane were calculated as follows, respectively [29]:

$$\%\eta = \frac{M}{M_0} \times 100 \tag{1}$$

$$F_W = \frac{V_W}{S.T} \tag{2}$$

where M_o and M are the masses of water before and after filtration, respectively. V_W , S, and T are the total volume of penetrating water (L), the operative membrane area (m²), and the process time (h), respectively.

3. Results and discussion

3.1 Preparation and characterization

The process of preparing GO/PVA-coated meshes is shown in Figure 1(a). After hydroxylation of SSL with HF solution, PVA polymer interacts with -OH of SSL via H-bond. Then, GA, as a crosslinking agent, interacts with the hydroxyl groups of PVA molecules and binds GO nanosheets on the surface of SSL [38]. Several oxygen-containing groups in GO easily interact with the cross-linked membrane. Herein, GO has an important role in enhancing hydrophilicity and surface roughness. PVA has excellent hydrophilicity and oil repellence properties. Hydrophilic GO/PVA nanocomposite on the surface of the membrane further enhances surface roughness and underwater oleophobicity in the hybrid membrane. Chemically cross-linked membranes showed improved stability due to strong interactions. The photographs of the pure and coated meshes are presented in Figure 1(b), which indicates the color change of the pure mesh after coating with GO/PVA nanocomposite.

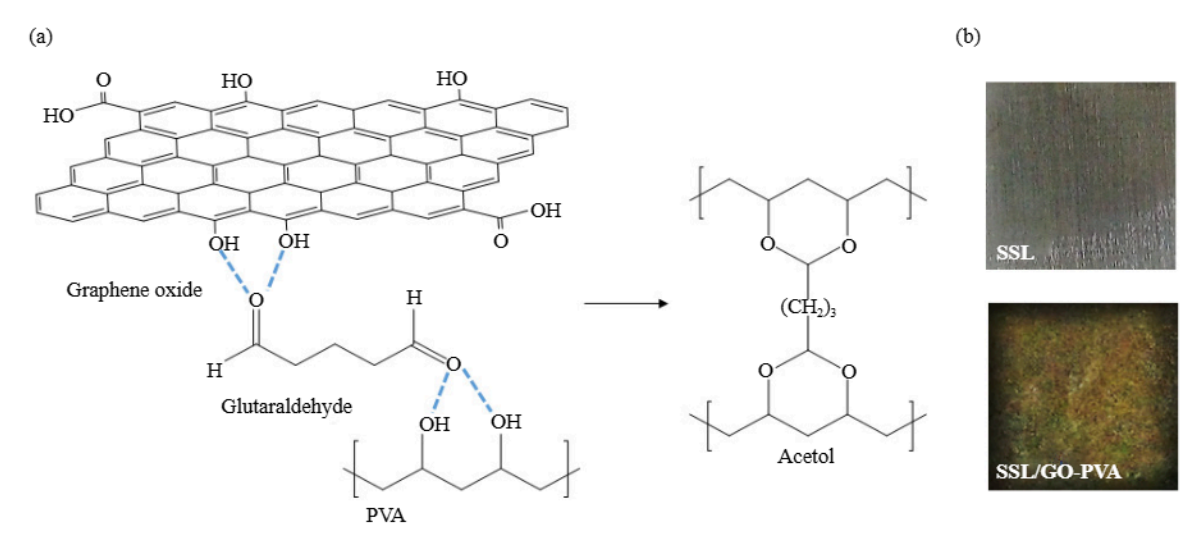


Figure 1. (a) The process of preparing GO/PVA-coated mesh; (b) photographic images of the pure (SSL) and coated (SSL/GO-PVA) meshes

The surface modification of SSL using the GO/PVA composite was verified by SEM. Figure $2(a_1-a_3)$ shows the smooth surface of the pure SSL with a pore diameter of about 50 μ m. After modification, the GO/PVA composite is fully covered in the surface of SSL and blocks the pores, as shown in Figure $2(b_1-b_3)$. The tiny pores on the coated SSL allow water to penetrate. It can be seen that GO/PVA composites are firmly stacked on the SSL surface as a nanoscale structure.

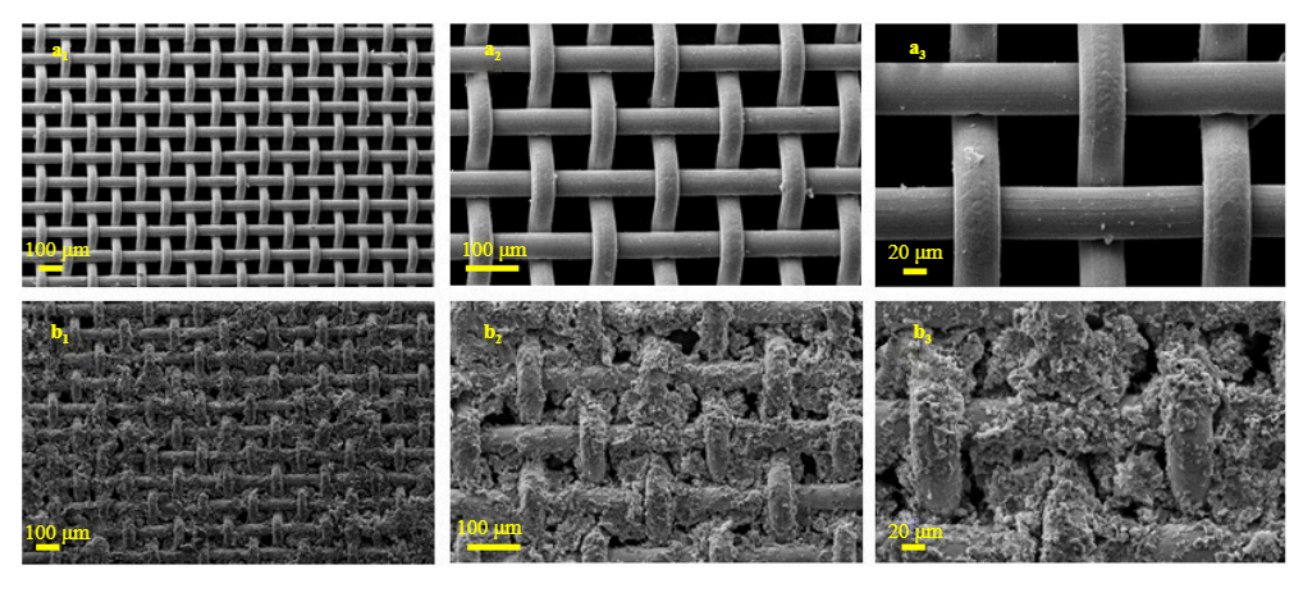


Figure 2. SEM images of (a1-a3) pure mesh and (b1-b3) GO/PVA-coated mesh

The FT-IR spectra of the pure and coated meshes are shown in Figure 3. After coating SSL, both characteristic bands of SSL and the GO/PVA composite were observed. Several characteristic bands located at 3,405, 2,942, 1,280, and 1,093 cm⁻¹ correspond to -OH, C-H, C-O, and C-C stretching vibrations in the GO/PVA composite, respectively. The -OH stretching at 3,437 cm⁻¹ in pure SSL and GO shifted to 3,405 cm⁻¹ after modification, indicating the strong hydrogen bond between SSL and PVA, which also confirmed the incorporation of GO in the polymer matrix and the formation of a hydrogen bond between GO and PVA. A characteristic band at 1,720 cm⁻¹ is attributed to aldehyde groups

in GO and GA. In the GO/PVA spectrum, the intensities of all the absorption bands correlated to the oxygen-containing groups increased.

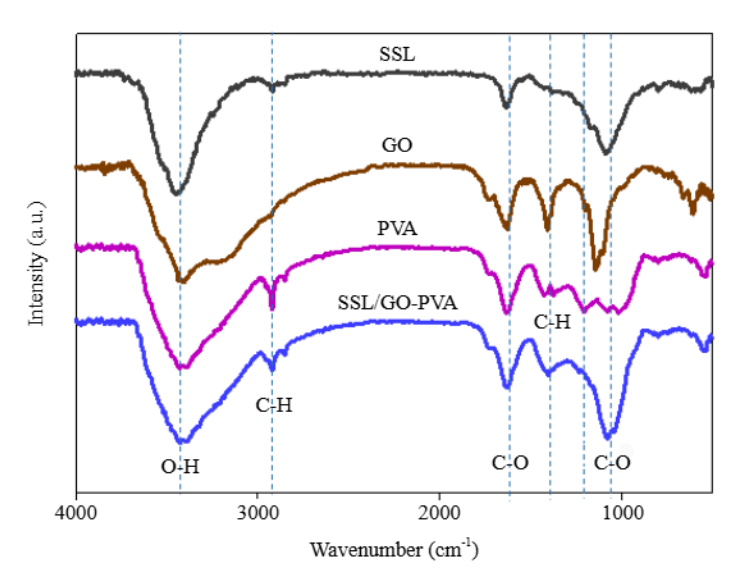


Figure 3. FTIR spectra of pure (SSL), GO, PVA, and SSL/GO-PVA

3.2 The wettability of the pure and coated mesh

The wetting properties of the pure and coated mesh were evaluated by dropping water and oil on the surface of the SSL and contact angle (CA) measurements. Both water and oil can penetrate through the pure mesh. As shown in Figure 4(a) and (b), an oil droplet on the pure mesh surface under water quickly spreads and permeates with CA of about 0°, while it remains spherical on the coated mesh surface, indicating the underwater oleophobic property of the coated mesh. The underwater oil CAs on the GO/PVA-coated meshes for different types of organic solvents are shown in Figure 4(c). Figure 4(c) shows that the underwater oil CAs for all types of organic solvents are about 150°. The underwater oil CAs of dichloromethane, toluene, and chloroform are 158°, 145°, and 151°, whereas the underwater oil CA of diesel is only 143°. These differences in oil CAs are possibly due to the variances in surface tension and intrinsic polarity of different types of oils [39].

The strong underwater superoleophobicity of the hybrid mesh is attributed to abundant oxygen-containing groups on the GO nanosheets, which can efficiently enhance the hydrophilicity so that a water layer can be trapped into the rough structures through hydrogen bonds, which avoid contacting oil with the surface of the mesh [40]. Therefore, the GO/PVA nanocomposite membrane shows excellent superhydrophilicity and underwater superoleophobicity.

In addition, the high underwater superoleophobicity of the coated mesh can be described by the Cassie model, as shown in Figure 4(d) [41]. When an oil droplet was preloaded on the mesh, it was easily detached from the mesh surface and maintained its spherical shape with no adhesion to the SSL surface (see Figure 4(e)). The results indicated the strong repellency of the coated mesh to oils.

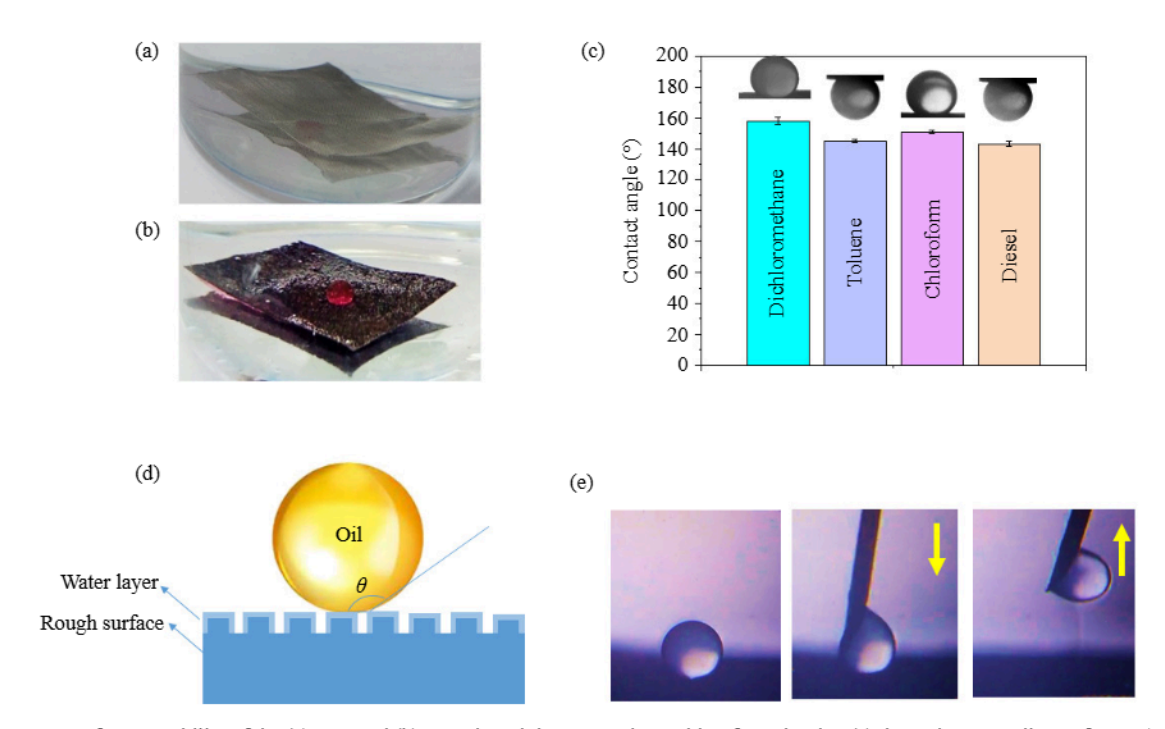


Figure 4. Surface wettability of the (a) pure and (b) coated mesh in water using a chloroform droplet; (c) the underwater oil CAs for GO/PVA nanocomposite membrane in various organic solvents; (d) a schematic of an oil droplet on a hierarchical structure (Cassie state); (e) the process of preloading and departing an oil droplet on the surface of the nanocomposite membrane

Jiang et al.'s model describes the underwater oil CA of a droplet on the solid surface by the following equation [42]:

$$\cos \theta_3 = \frac{\gamma_{o-\alpha} \cos \theta_1 - \gamma_{w-\alpha} \cos \theta_2}{\gamma_{o-w}}$$

where θ_1 , θ_2 , and θ_3 are the oil CA in air, the water CA in air, and the oil CA in water, respectively. γ_{o-a} , γ_{w-a} , and γ_{o-w} are the oil/air, water/air, and oil/water interface tensions. Generally, the values of γ_{o-a} are in the range of 20 to 30 mN m⁻¹ and γ_{w-a} is 73 mN m⁻¹ [43]. Since θ_1 is usually near 0°, decreasing θ_2 results in a larger θ_3 ; in other words, an increase in the hydrophilicity of the substrate leads to an enhancement in underwater oleophobicity. In this work, by coating a hydrophilic GO film on the mesh surface, θ_2 decreases, thus the underwater oil CAs (θ_3) increase.

3.3 Oil/water separation experiment

The oil/water mixture separation performance of the GO/PVA mesh was examined by passing the oil-water mixture onto the mesh placed between two tubes. Due to its superhydrophilicity, water quickly passed through the membrane by gravity with a high water flux, and the oil was trapped on the membrane surface regarding its underwater superoleophobic property (Figure 5(a)). No visible red-colored oil was detected in the collected water, confirming the superior separation efficiency of the coated mesh. The separation efficiencies and water flux for various types of oil/water mixtures are shown in Figure 5(b). The separation efficiencies and water flux for all mixtures are higher than 97.8% and $6000.0 \text{ L m}^{-2} \text{ h}^{-1}$, respectively.

In gravity-driven oil/water mixture separation, intrusion pressure plays an important role. The intrusion pressure was measured to determine the liquid-holding capacity of the nanocomposite membrane. For this purpose, selected oil is continuously added to the membrane until its pressure reaches a threshold such that the oil begins to permeate through the membrane pores. The oil intrusion pressure (*P*) was obtained by the following equation [27]:

$$P = \rho_{oil} g h_{max} \tag{4}$$

where, ρ_{oil} is the oil density (kg/m³), g is the acceleration of gravity (9.80 m/s²), and h_{max} is the maximum oil height that the mesh can withstand (m), respectively. The h_{max} for toluene was obtained at about 13.1 cm with an oil intrusion pressure of 1.11 kPa, indicating efficient separation of the oil/water mixture using a GO/PVA nanocomposite membrane.

The recyclability of the GO/PVA nanocomposite membrane was evaluated by performing the experiment in a chloroform/water mixture for 20 cycles (Figure 5(c)). The separation efficiencies of the proposed membrane for the chloroform/water mixture were above 97.0% without obvious decay after 20 cycles. The high separation efficiency can be due to the mutual effects of micro- and nanostructuring on the membrane surface and the high hydrophilicity of the nanocomposite membrane, which is comparable to or even superior to some reported studies [28, 44, 45].

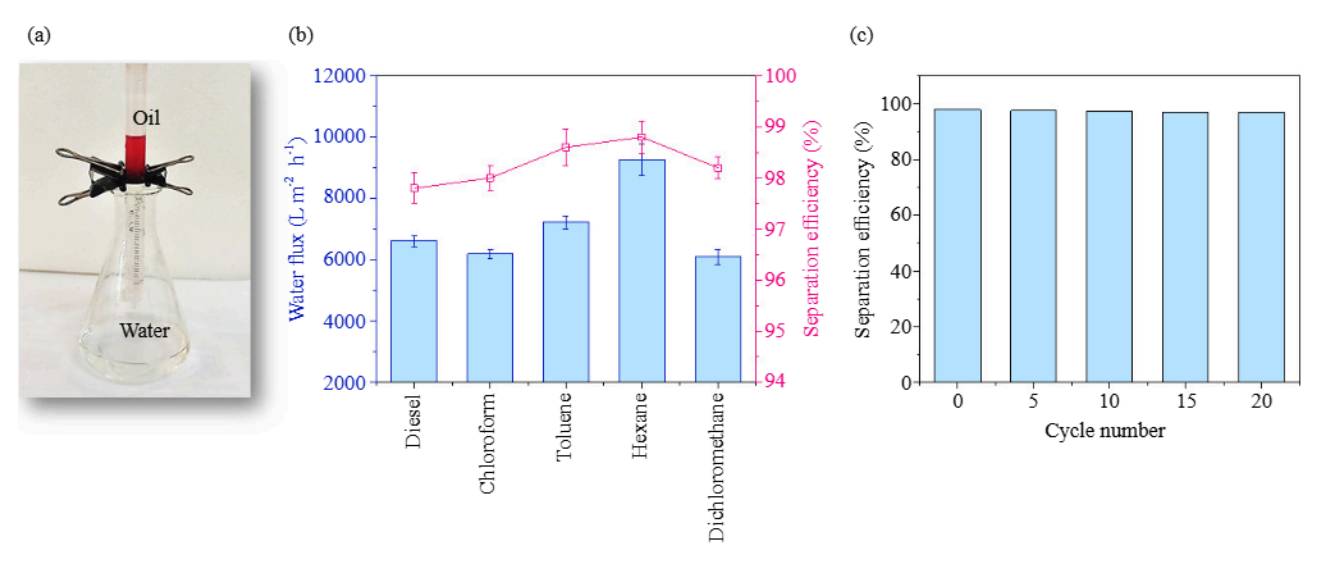


Figure 5. (a) The oil/water mixture separation; (b) the separation efficiency (right) and water flux (left) for various kinds of oil/water mixture; (c) the recyclability test of the GO/PVA nanocomposite membrane for chloroform/water mixture

3.4 Stability test

In practical industrial applications, the separation of oil/water mixture is often implemented in various harsh environments. Therefore, the chemical stability of the GO/PVA nanocomposite membrane was estimated in various harsh environments, including basic, acidic, or saline solutions, by measuring the oil CAs. The underwater oil CAs were measured after immersion in 1 M HCl, 1 M NaOH, and a 10% NaCl solution for 48 h. As shown in Figure 6, the underwater oil CAs of a chloroform droplet on the membrane surface under different harsh conditions are more than 145°, implying excellent chemical stability of the coated membrane.

Additionally, the stability of the nanocomposite membrane was evaluated by an abrasion resistance test. The experiment was studied by dragging a coated mesh onto 1,500 mesh sandpaper under a weight of 100 g and 20 cm of pulling back and forth for 10 cycles. After each cycle, the oil CAs were measured. As shown in Figure 6(b), oil CA changes in an oil droplet are insignificant after 10 abrasion cycles, indicating good abrasion resistance and high stability of the nanocomposite membrane can be attributed to the strong crosslinking effect induced by PVA polymers and GA.

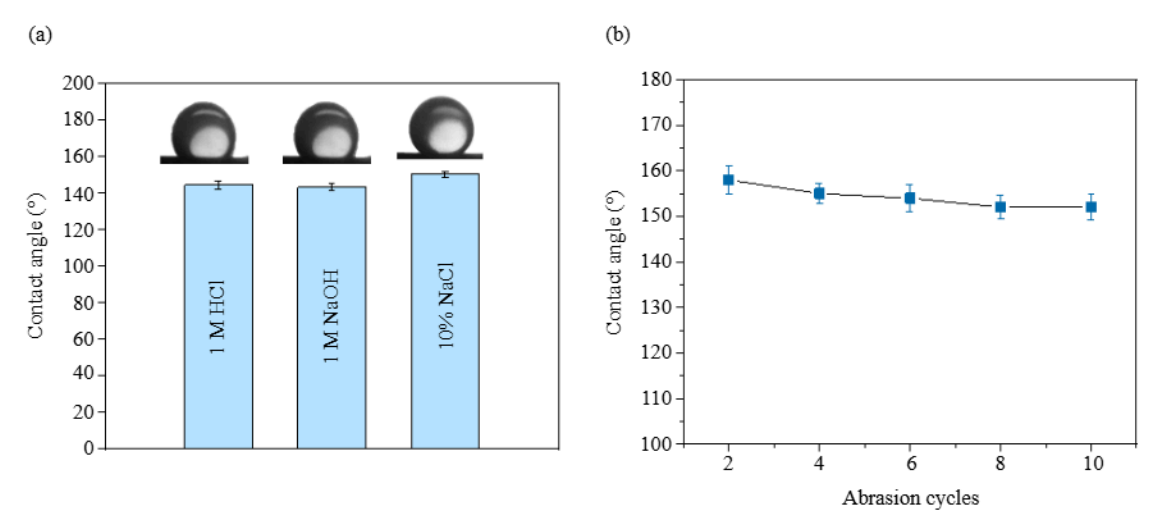


Figure 6. (a) The variation in the underwater oil CAs for the GO/PVA nanocomposite membrane in different harsh conditions; (b) the oil CAs of an oil droplet for ten abrasion cycles

4. Conclusion

The GO/PVA nanocomposite membrane was prepared via a cross-linking reaction. The hierarchical rough structure and hydrophilic nature of the GO/PVA nanocomposite resulted in the superwetting membrane. The asprepared membrane can effectively separate a variety of oil/water mixtures with separation efficiency and water flux above 97.8% and 6000.0 L m⁻² h⁻¹, respectively. The oil intrusion pressure was 1.1 kPa, indicating the highly efficient oil/water separation capability of the nanocomposite membrane. In addition, the GO/PVA nanocomposite membrane showed good recyclability after 20 cycles and high stability in acidic, basic, and saline solutions. The results also showed the high abrasion resistance of the prepared membrane after 10 cycles. Due to the outstanding properties of the prepared membrane, such as its simple preparation technique and chemical stability, this membrane might be used in real environments with harsh conditions. It should be noted that real samples might have higher densities of oil than those used in our experiments. Given that superoleophobic membranes are more suitable for light oil-water separation, much effort needs to be allocated to the development of new materials that are also appropriate for the separation of high-density oils. Considering the properties of GO, the development of novel composite materials using GO leads to improvements in the field of water purification.

Acknowledgment

The authors acknowledge the financial support from Ferdowsi University of Mashhad for a post-doctoral fellowship.

Conflict of interest

The authors declare that there is no conflict of interest regarding the publication of this paper.

References

- [1] Zhang N, Qi Y, Zhang Y, Luo J, Cui P, Jiang W. A review on oil/water mixture separation material. *Industrial & Engineering Chemistry Research*. 2020; 59: 14546-14568. https://doi.org/10.1021/acs.iecr.0c02524
- [2] Nam C, Li H, Zhang G, Lutz LR, Nazari B, Colby RH, et al. Practical oil spill recovery by a combination of

- polyolefin absorbent and mechanical skimmer. ACS Sustainable Chemical Engineering. 2018; 6: 12036-12045. https://doi.org/10.1021/acssuschemeng.8b02322
- [3] Abidli A, Huang Y, Cherukupally P, Bilton AM, Park CB. Novel separator skimmer for oil spill cleanup and oily wastewater treatment: From conceptual system design to the first pilot-scale prototype development. *Environmental Technology and Innovation*. 2020; 18: 100598. https://doi.org/10.1016/j.eti.2019.100598
- [4] Kong D, He X, Yang H, Zhang Z. Experimental study for flame base drag and burning efficiency of spilled crude oil during in-situ burning on water. *Process Safety and Environmental Protection*. 2019; 131: 48-54. https://doi.org/10.1016/j.psep.2019.08.006
- [5] Jaggi A, Radović JR, Snowdon LR, Larter SR, Oldenburg TBP. Composition of the dissolved organic matter produced during in situ burning of spilled oil. *Organic Geochemistry*. 2019; 138: 103926. https://doi.org/10.1016/ j.orggeochem.2019.103926
- [6] Piccioli M, Aanesen SV, Zhao H, Dudek M, Øye G. Gas flotation of petroleum produced water: A review on status, fundamental aspects, and perspectives. *Energy & Fuels*. 2020; 34(12): 15579. https://doi.org/10.1021/acs. energyfuels.0c03262
- [7] Wang C, Lü Y, Song C, Zhang D, Rong F, He L. Separation of emulsified crude oil from produced water by gas flotation: A review. Science of The Total Environment. 2022; 845: 157304. https://doi.org/10.1016/ j.scitotenv.2022.157304
- [8] Davardoostmanesh M, Ahmadzadeh H. A mechanically flexible superhydrophobic rock wool modified with reduced graphene oxide-chloroperene rubber for oil-spill clean-up. *Global Challenges*. 2021; 5(12): 2100072. https://doi.org/10.1002/gch2.202100072
- [9] Ding F, Gao M. Pore wettability for enhanced oil recovery, contaminant adsorption and oil/water separation: A review. Advances in Colloid and Interface Science. 2021; 289: 102377. https://doi.org/10.1016/j.cis.2021.102377
- [10] Padaki M, Surya Murali R, Abdullah MS, Misdan N, Moslehyani A, Kassim MA, et al. Membrane technology enhancement in oil-water separation. A review. *Desalination*. 2015; 357: 197-207. https://doi.org/10.1016/ j.desal.2014.11.023
- [11] Wei Y, Qi H, Gong X, Zhao S. Specially wettable membranes for oil-water separation. *Advanced Materials Interfaces*. 2018; 5(23): 1800576. https://doi.org/10.1002/admi.201800576
- [12] Asadpour R, Yavari S, Kamyab H, Ashokkumar V, Chelliapan S, Yuzir A. Study of oil sorption behaviour of esterified oil palm empty fruit bunch (OPEFB) fibre and its kinetics and isotherm studies. *Environmental Technology & Innovation*. 2021; 22: 101397. https://doi.org/10.1016/j.eti.2021.101397
- [13] Baig U, Faizan M, Sajid M. Multifunctional membranes with super-wetting characteristics for oil-water separation and removal of hazardous environmental pollutants from water: A review. *Advances in Colloid and Interface Science*. 2020; 285: 102276. https://doi.org/10.1016/J.CIS.2020.102276
- [14] Rasouli S, Rezaei N, Hamedi H, Zendehboudi S, Duan X. Superhydrophobic and superoleophilic membranes for oil-water separation application: A comprehensive review. *Material & Design*. 2021; 204: 109599. https://doi. org/10.1016/j.matdes.2021.109599
- [15] Baig U, Dastageer MA, Gondal MA. Facile fabrication of super-wettable mesh membrane using locally-synthesized cobalt oxide nanoparticles and their application in efficient gravity driven oil/water separation. Colloids and Surfaces A: Physicochemical and Engineering Aspect. 2023; 660: 130793. https://doi.org/10.1016/ J.COLSURFA.2022.130793
- [16] Davardoostmanesh M, Ahmadzadeh H. Remediation of saline oily water using an algae-based membrane. *Journal of Membrane Science*. 2023; 666: 121201. https://doi.org/10.1016/J.MEMSCI.2022.121201
- [17] Liu Y, Wang L, Lu H, Huang Z. Achieving effective oil/water separation with bicomponent supramolecular hydrogel paint coated metal mesh. ACS Applied Polymer Materials. 2020; 2(11): 4770-4778. https://doi. org/10.1021/acsapm.0c00764
- [18] Wang R, Zhu L, Zhu X, Yan Z, Xia F, Zhang J, et al. A super-hydrophilic and underwater super-oleophobic membrane with robust anti-fouling performance of high viscous crude oil for efficient oil/water separation. Colloids and Surfaces A: Physicochemical and Engineering Aspect. 2023; 658: 130662. https://doi.org/10.1016/ J.COLSURFA.2022.130662
- [19] Li H, Yin Y, Zhu L, Xiong Y, Li X, Guo T, et al. A hierarchical structured steel mesh decorated with metal organic framework/graphene oxide for high-efficient oil/water separation. *Journal of Hazardous Materials*. 2019; 373: 725-732. https://doi.org/10.1016/j.jhazmat.2019.04.009
- [20] Zhu M, Liu Y, Chen M, Sadrzadeh M, Xu Z, Gan D, et al. Robust superhydrophilic and underwater superoleophobic membrane optimized by Cu doping modified metal-organic frameworks for oil-water separation and water purification. *Journal of Membrane Science*. 2021; 640: 119755. https://doi.org/10.1016/

J.MEMSCI.2021.119755

- [21] Pan J, Ge Y. Low-cost and high-stability superhydrophilic/underwater superoleophobic NaA zeolite/copper mesh composite membranes for oil/water separation. *Surfaces and Interfaces*. 2023; 37: 102703. https://doi.org/10.1016/ j.surfin.2023.102703
- [22] Cao L, Zhou J, Hao H, Dutta PK. High-flux, efficient and reusable zeolite/stainless steel meshes for oil/ water separation. *Microporous Mesoporous Materials*. 2022; 336: 111870. https://doi.org/10.1016/ j.micromeso.2022.111870
- [23] Liu Y-Q, Zhang Y-L, Fu X-Y, Sun H-B. Bioinspired underwater superoleophobic membrane based on a graphene oxide coated wire mesh for efficient oil/water separation. ACS Applied Materials & Interfaces. 2015; 7(37): 20930-20936. https://doi.org/10.1021/acsami.5b06326
- [24] Tian X, Tian S, Wang L, Yang Y, Zhang R, Dai J, et al. Underwater superoleophobic GO-PEI-SiO₂-Hal quaternary sphere-rod nacre-inspired mesh by LBL self-assembly for high-efficiency oil-water separation. *Applied Clay Science*. 2023; 232: 106772. https://doi.org/10.1016/J.CLAY.2022.106772
- [25] Liu M, Wang S, Wei Z, Song Y, Jiang L. Bioinspired design of a superoleophobic and low adhesive water/solid interface. Advanced Materials. 2009; 21(6): 665-669. https://doi.org/10.1002/adma.200801782
- [26] Chen J, Li K, Zhang H, Liu J, Wu S, Fan Q, et al. Highly efficient and robust oil/water separation materials based on wire mesh coated by reduced graphene oxide. *Langmuir*. 2017; 33(38): 9590-9597. https://doi.org/10.1021/acs. langmuir.7b01856
- [27] Chen C, Chen B. Graphene oxide coated meshes with stable underwater superoleophobicity and anti-oil-fouling property for highly efficient oil/water separation. *Science of The Total Environment*. 2019; 696: 133777. https://doi.org/10.1016/j.scitotenv.2019.133777
- [28] Lu H, Sha S, Yang S, Wu J, Ma J, Hou C, et al. The coating and reduction of graphene oxide on meshes with inverse wettability for continuous water/oil separation. *Applied Surface Science*. 2021; 538: 147948. https://doi. org/10.1016/j.apsusc.2020.147948
- [29] Wang L, Wang Y, Dai J, Tian S, Xie A, Dai X, et al. Coordination-driven interfacial cross-linked graphene oxide-alginate nacre mesh with underwater superoleophobicity for oil-water separation. *Carbohydrate Polymers*. 2021; 251: 117097. https://doi.org/10.1016/j.carbpol.2020.117097
- [30] Alammar A, Park SH, Williams CJ, Derby B, Szekely G. Oil-in-water separation with graphene-based nanocomposite membranes for produced water treatment. *Journal of Membrane Science*. 2020; 603: 118007. https://doi.org/10.1016/J.MEMSCI.2020.118007
- [31] Dong Y, Li J, Shi L, Wang X, Guo Z, Liu W. Underwater superoleophobic graphene oxide coated meshes for the separation of oil and water. *Chemical Communications*. 2014; 50(42): 5586-5589. https://doi.org/10.1039/ C4CC01408A
- [32] Dai J, Wang L, Wang Y, Tian S, Tian X, Xie A, et al. Robust nacrelike graphene oxide-calcium carbonate hybrid mesh with underwater superoleophobic property for highly efficient oil/water separation. *ACS Applied Materials & Interfaces*. 2020; 12(4): 4482-4493. https://doi.org/10.1021/acsami.9b18664
- [33] Jaleh B, Shariati K, Khosravi M, Moradi A, Ghasemi S, Azizian S. Uniform and stable electrophoretic deposition of graphene oxide on steel mesh: Low temperature thermal treatment for switching from superhydrophilicity to superhydrophobicity. *Colloids and Surfaces A: Physicochemical and Engineering Aspect.* 2019; 577: 323-332. https://doi.org/10.1016/j.colsurfa.2019.05.085
- [34] Yang E, Kim C-M, Song J, Ki H, Ham M-H, Kim IS. Enhanced desalination performance of forward osmosis membranes based on reduced graphene oxide laminates coated with hydrophilic polydopamine. *Carbon.* 2017; 117: 293-300. https://doi.org/10.1016/j.carbon.2017.03.005
- [35] Zhang T, Xiao C, Zhao J, Liu X, Ji D, Zhang H. One-step facile fabrication of PVDF/graphene composite nanofibrous membrane with enhanced oil affinity for highly efficient gravity-driven emulsified oil/water separation and selective oil absorption. *Separation and Purification Technology*. 2021; 254: 117576. https://doi.org/10.1016/j.seppur.2020.117576
- [36] Yin Y, Li H, Zhu L, Guo T, Li X, Xing W, et al. A durable mesh decorated with polydopamine/graphene oxide for highly efficient oil/water mixture separation. *Applied Surface Science*. 2019; 479: 351-359. https://doi.org/10.1016/ j.apsusc.2019.01.118
- [37] Huang T, Zhang L, Chen H, Gao C. Sol-gel fabrication of a non-laminated graphene oxide membrane for oil/water separation. *Journal of Materials Chemistry A.* 2015; 3(38): 19517-19524. https://doi.org/10.1039/C5TA04471E
- [38] Zhu X, Tang X, Luo X, Yang Z, Cheng X, Gan Z, et al. Stainless steel mesh supported thin-film composite nanofiltration membranes for enhanced permeability and regeneration potential. *Journal of Membrane Science*. 2021; 618: 118738. https://doi.org/10.1016/j.memsci.2020.118738

- [39] He H, Li Z, Ouyang L, Liang Y, Yuan S. Hierarchical WO₃@Cu(OH)₂ nanorod arrays grown on copper mesh with superwetting and self-cleaning properties for high-performance oil/water separation. *Journal of Alloys and Compounds*. 2021; 855(Part 2): 157421. https://doi.org/10.1016/j.jallcom.2020.157421
- [40] Liu Y, Zhang F, Zhu W, Su D, Sang Z, Yan X, et al. A multifunctional hierarchical porous SiO₂/GO membrane for high efficiency oil/water separation and dye removal. *Carbon*. 2020; 160: 88-97. https://doi.org/10.1016/j.carbon.2020.01.002
- [41] An S, Joshi BN, Lee J-G, Lee MW, Kim YI, Kim M, et al. A comprehensive review on wettability, desalination, and purification using graphene-based materials at water interfaces. *Catalysis Today*. 2017; 295: 14-25. https://doi.org/10.1016/j.cattod.2017.04.027
- [42] Li J-J, Zhou Y-N, Luo Z-H. Polymeric materials with switchable superwettability for controllable oil/water separation: A comprehensive review. *Progress in Polymer Science*. 2018; 87: 1-33. https://doi.org/10.1016/j.progpolymsci.2018.06.009
- [43] Wang H, Hu X, Ke Z, Du CZ, Zheng L, Wang C, et al. Review: Porous metal filters and membranes for oil-water separation. *Nanoscale Research Letters*. 2018; 13: 284. https://doi.org/10.1186/s11671-018-2693-0
- [44] Liu Y, Zhang K, Yao W, Zhang C, Han Z, Ren L. A facile electrodeposition process for the fabrication of superhydrophobic and superoleophilic copper mesh for efficient oil-water separation. *Industrial & Engineering Chemistry Research*. 2016; 55(10): 2704. https://doi.org/10.1021/acs.iecr.5b03503
- [45] Pi P, Hou K, Zhou C, Li G, Wen X, Xu S, et al. Superhydrophobic Cu₂S@Cu₂O film on copper surface fabricated by a facile chemical bath deposition method and its application in oil-water separation. *Applied Surface Science*. 2017; 396: 566-573. https://doi.org/10.1016/j.apsusc.2016.10.198